

# Quantifying ground-state complexation between $\text{Ag}^+$ and polycyclic aromatic hydrocarbons in dilute aqueous solution via fluorescence quenching

Ji Hoon Lee<sup>a</sup>, Mark A. Schlautman<sup>a,b,\*</sup>, Elizabeth R. Carraway<sup>a,b,1</sup>,  
Soobin Yim<sup>a</sup>, Bruce E. Herbert<sup>c</sup>

<sup>a</sup> Clemson Institute of Environmental Toxicology, Clemson University, Pendleton, SC 29670, USA

<sup>b</sup> School of the Environment, Clemson University, Clemson, SC 29634-0919, USA

<sup>c</sup> Department of Geology and Geophysics, Texas A&M University, College Station, TX 77843, USA

Received 30 July 2003; received in revised form 11 November 2003; accepted 20 November 2003

## Abstract

Interactions of  $\text{Ag}^+$  with naphthalene and pyrene in aqueous solution were investigated using ultraviolet (UV) absorption and steady-state and time-resolved fluorescence spectroscopies. Small red-shifts in the two primary absorption bands of naphthalene and pyrene were observed in the presence of high concentrations of  $\text{Ag}^+$ , indicating that ground-state cation–aromatic  $\pi$  electron interactions occurred.  $\text{Ag}^+$  complexation constants ( $K_1$  and  $K_2$ ) for naphthalene were determined directly from steady-state and time-resolved fluorescence data, whereas the formation of a pyrene– $\text{Ag}^+$  exciplex required an additional correction to remove its interference on apparent pyrene complexation constants. The correction utilized ratios of the exciplex and monomer preexponential factors obtained from pyrene fluorescence decay curves measured at several emission wavelengths that were impacted to different degrees by the exciplex emission. The novel approach developed here to quantify ground-state complexes between  $\text{Ag}^+$  and polycyclic aromatic hydrocarbons (PAHs) offers new opportunities to investigate weak metal–organic complexes such as those resulting from cation– $\pi$  interactions.

© 2004 Elsevier B.V. All rights reserved.

**Keywords:** Pyrene; Naphthalene; Silver ion; Metal complexation; Dynamic quenching; Exciplex; Time-resolved fluorescence; Steady-state fluorescence

## 1. Introduction

Ever since single ring aromatic compounds were reported to form 1:1 complexes with silver ions [1–3], polycyclic aromatic hydrocarbons (PAHs) have been recognized as potential donor molecules for preparing  $\text{Ag}^+$ –aromatic  $\pi$  complexes in aqueous [4–7] and organic solvents [5,8,9]. The  $\text{Ag}^+$ –aromatic  $\pi$  interaction has also been studied in gas [10,11] and solid [12–18] phases. Mulliken [19] formulated a theoretical model for the bonding between silver perchlorate and benzene and Fukui et al. [20] provided a molecular orbital theoretical treatment of the electronic requirements of  $\text{Ag}^+$ –aromatic  $\pi$  interactions. Based on these results [19,20], cation–aromatic  $\pi$  interactions are

expected to consist of charge–quadrupole, charge–dipole, charge–induced dipole, charge transfer, dispersion force, electrostatic interaction, and hydrophobic components. Recently, Munakata et al. [21] provided a review on the formation of  $\text{Ag}^+$  ion–PAH complexes in various phases.

Andrews and Keefer [4] suggested that the water soluble aromatic  $\pi$  complexes  $\text{AgAr}^+$  and  $\text{Ag}_2\text{Ar}^{2+}$  are in equilibrium with the aromatic compound and free  $\text{Ag}^+$ , and that the monosilver complex is predominant in the ground-state. In other words, the complexation constant for  $\text{Ag}_2\text{Ar}^{2+}$  is a minor component in calculating the overall speciation. Kofahl and Lucas [5] determined  $\text{Ag}^+$  complexation constants of various PAHs in an aqueous medium containing  $\text{KNO}_3$  and  $\text{AgNO}_3$  at unit ionic strength and in equimolar water–methanol solutions containing  $\text{NaNO}_3$  and  $\text{AgNO}_3$  at ionic strength 0.5 using a solubility enhancement method. They found that  $\text{Ag}^+$  complexation constants of phenanthrene (Phen) depended significantly on the polarity of the solvent systems. For example, the complexation constant for formation of  $\text{AgPhen}^+$  in aqueous medium was 3.3

\* Corresponding author. Tel.: +1-864-656-4059; fax: +1-864-656-0672.

E-mail addresses: [mschlau@clemson.edu](mailto:mschlau@clemson.edu) (M.A. Schlautman), [ecarraw@clemson.edu](mailto:ecarraw@clemson.edu) (E.R. Carraway).

<sup>1</sup> Co-corresponding author. Tel.: +1-864-646-2189; fax: +1-864-646-2277.

times larger than that obtained in the water–methanol system [5]. Recently, Yim [7] determined  $\text{Ag}^+$  complexation constants for naphthalene (Naph), pyrene (Pyr), and perylene (Peryl) using a similar solubility enhancement technique and showed that the constants increased proportionally with increasing molar volume and reduction potential [22,23] of the PAHs (e.g. Naph < Pyr < Peryl). Zhu et al. [24] recently demonstrated that  $\text{Ag}^+$  complexation constants for deuterated aromatic molecules can be determined via deuterium nuclear magnetic resonance spin–lattice relaxation ( $^2\text{H}$  NMR  $T_1$ ) measurements, thereby eliminating the need to conduct solubility enhancement studies which can be confounded by macroscopic salting out effects [7].

In this paper, we demonstrate that quenching of PAH fluorescence by  $\text{Ag}^+$  ions can be used to quantify their  $\text{Ag}^+$  complexation constants in dilute aqueous solution. Because of its inherent sensitivity, fluorescence quenching alleviates many of the problems previously associated with obtaining  $\text{Ag}^+$  complexation constants from solubility enhancement methodologies (e.g. salting out effects, need for high  $\text{Ag}^+$  concentrations) and even  $^2\text{H}$  NMR  $T_1$  measurements (e.g. method sensitivity limitations, aromatic compound solubility limitations, need for high  $\text{Ag}^+$  concentrations). In addition, the fluorescence quenching technique is simple and rapid compared to traditional solubility enhancement methodologies.

## 2. Experimental

### 2.1. Chemicals

$\text{AgClO}_4$  (99.9%),  $\text{NaClO}_4$  (99.0%), naphthalene (99.0%), and pyrene (99.0%) were purchased from Aldrich and used without further purification. Spectroscopic grade methanol was purchased from Fisher Scientific. Distilled, deionized water (Super-Q<sup>TM</sup> Plus, Millipore) having a resistivity greater than  $18.0\text{ M}\Omega\text{ cm}$  was used to prepare all aqueous solutions.

### 2.2. General procedures

Naphthalene, pyrene, and  $\text{AgClO}_4$  stock solutions were prepared at room temperature ( $21 \pm 2^\circ\text{C}$ ) and stored in dark containers to minimize photoreactions. Samples for absorption and fluorescence measurements were prepared in an anaerobic chamber (95%  $\text{N}_2$ , 5%  $\text{H}_2$ ; Coy Laboratory Products Inc.) using deoxygenated solvents and then sealed in 1 cm screw cap anaerobic fluorescence cells (Starna) to exclude oxygen. The ionic strength of most samples was fixed at 0.1 M with  $\text{NaClO}_4$ , except for some ultraviolet (UV) absorption measurements conducted at relatively high  $\text{Ag}^+$  concentrations (0.15–0.3 M) to detect its interactions with naphthalene and pyrene. In general,  $\text{Na}^+$  and  $\text{ClO}_4^-$  are not considered to be quenchers of PAH fluorescence [25]. Also,  $\text{AgClO}_4$  and  $\text{NaClO}_4$  solution have no apprecia-

ble absorption bands in the wavelength region longer than 300 nm [9].

UV-Vis absorption spectra (resolution of 0.05 nm) were measured with a double-beam, double-monochromator spectrophotometer (Shimadzu UV-2501PC) using appropriate background solutions as references. Steady-state fluorescence spectra were recorded with a PTI QuantaMaster<sup>TM</sup> spectrometer (Photon Technology International, Inc.) equipped with a 75 W xenon arc lamp. The excitation wavelengths used for naphthalene and pyrene were 276 and 334 nm, respectively. Fluorescence emission was monitored at 322 nm for naphthalene, while pyrene emission was monitored at 373, 379, 383, and 393 nm. Excitation and emission slits were adjusted to a resolution of 0.25 nm. When necessary, observed fluorescence intensities were corrected for inner filter effects and/or Raman scattering from the background solution [26,27]. Fluorescence lifetimes at the same emission wavelengths above were obtained with a PTI TimeMaster<sup>TM</sup> spectrometer using a nitrogen-filled nanosecond flashlamp and a stroboscopic optical boxcar detection methodology. Lifetime data analyses were performed using TimeMaster Pro<sup>TM</sup> for Windows provided with the PTI system. Observed fluorescence decays were deconvoluted using a sum of exponentials model and a measured excitation pulse by the Marquardt nonlinear least-squares method. For pyrene, both monomer and exciplex emission decay lifetimes in the presence of  $\text{AgClO}_4$  were determined at each wavelength. Goodness of fit was characterized by the reduced chi-square statistic ( $\chi^2$ ), Durbin–Watson parameter, runs test, and plots of the weighted residuals and autocorrelation function of weighted residuals. Best fit values for the lifetimes ( $\tau_i$ ) and/or preexponential factors ( $A_i$ ) were then used in subsequent calculations and analyses.

## 3. Results and discussion

### 3.1. Absorption spectra

Relatively high concentrations of  $\text{Ag}^+$  in aqueous solution resulted in UV spectra for naphthalene and pyrene that were slightly red-shifted compared to spectra observed in the absence of  $\text{Ag}^+$  ions (Fig. 1). For example, the presence of 0.30 M  $\text{Ag}^+$  ions generated red-shifts of approximately 1 nm in the two primary absorption bands (266 and 276 nm) of naphthalene (Fig. 1A). Similar red-shifts occurred for pyrene at 319 and 334 nm in the presence of 0.15 M  $\text{Ag}^+$  (Fig. 1B). The trends of the two curves shown in Fig. 1B are similar to those observed in the absorption spectra of caffeine-solubilized pyrene in aqueous solution in the absence and presence of  $\text{AgNO}_3$  [28]. Fig. 1 provides suggestive evidence that cation–aromatic  $\pi$  electron interactions between  $\text{Ag}^+$  ions and PAH molecules occur in the ground-state, even though the relevant absorption bands of the complexes formed overlay the local bands of the aromatic donors [29]. Unfortunately, the very small absorption

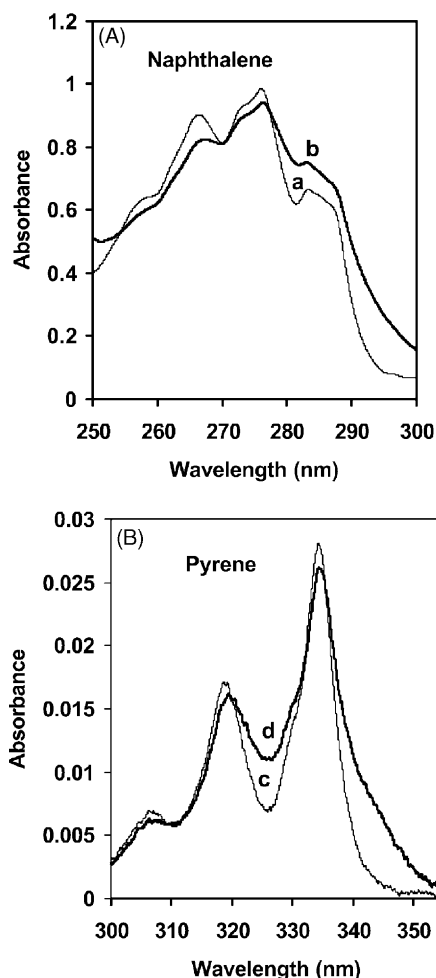


Fig. 1. (A) Absorption spectra of naphthalene ( $2.0 \times 10^{-4}$  M) in aqueous solution ( $I = 0.30$  M) for 0 (a), and 0.30 M (b)  $\text{AgClO}_4$ . Reference solutions for curves (a) and (b) were 0.30 M  $\text{NaClO}_4$  and 0.30 M  $\text{AgClO}_4$ , respectively. The presence of weak naphthalene– $\text{Ag}^+$  complexes are indicated by the slight red-shifts in the absorption bands at 266 and 276 nm in curve (b). (B) Absorption spectra of pyrene ( $4.5 \times 10^{-7}$  M) in aqueous solution ( $I = 0.15$  M) for 0 (c) and 0.15 M (d)  $\text{AgClO}_4$ . Reference solutions for curves (c) and (d) were 0.15 M  $\text{NaClO}_4$  and 0.15 M  $\text{AgClO}_4$ , respectively. The presence of weak pyrene– $\text{Ag}^+$  complexes are indicated by the slight red-shifts in the absorption bands at 319 and 334 nm in curve (d).

band shifts observed coupled with the relatively low sensitivity of the UV-Vis spectrophotometer did not allow for  $\text{Ag}^+$  complexation constants to be calculated for naphthalene and pyrene in these systems.

### 3.2. Dynamic and steady-state fluorescence measurements for naphthalene

For this study, fluorescence techniques proved to be much more sensitive than UV-Vis absorption because  $\text{Ag}^+$  is known to be a strong quencher of PAH fluorescence [27]. Fig. 2A shows that  $\text{Ag}^+$  is both a static and dynamic quencher of naphthalene fluorescence in aqueous solution.

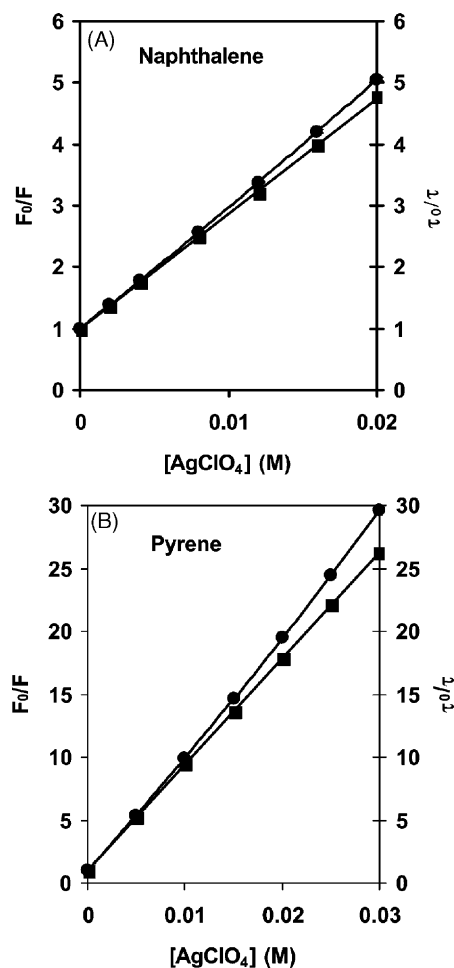


Fig. 2. Representative Stern–Volmer plots for the steady-state (●) and time-resolved (■) fluorescence quenching of (A) naphthalene ( $[\text{Naph}] = 2.0 \times 10^{-4}$  M,  $\lambda_{\text{em}} = 322$  nm) and (B) pyrene ( $[\text{Pyr}] = 4.5 \times 10^{-7}$  M,  $\lambda_{\text{em}} = 373$  nm) by  $\text{Ag}^+$ .

Although dynamic quenching by  $\text{Ag}^+$  is predominant, the static quenching component can be resolved and indicates that  $\text{Ag}^+$  ions interact with the diffuse  $\pi$  electron clouds of naphthalene to form complexes in the ground-state. Therefore, the steady-state Stern–Volmer equation is second-order with respect to  $\text{Ag}^+$  ion concentration [27]:

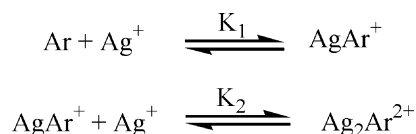
$$\frac{F_0}{F} = (1 + K_D[Q])(1 + K_S[Q]) \quad (1)$$

where  $F_0$  and  $F$  are the steady-state fluorescence intensities in the absence and presence of  $\text{Ag}^+$  ions, respectively,  $[Q]$  is the  $\text{Ag}^+$  (quencher) concentration, and  $K_D$  and  $K_S$  are the dynamic and static quenching constants, respectively.  $K_D$  is generally considered to be the product of the bimolecular fluorescence quenching rate constant ( $k_q$ ) and the naphthalene fluorescence lifetime ( $\tau_0$ ) [27], while  $K_S$  is normally reported to be for a 1:1 complex [27]:

$$K_S = \frac{[\text{Ar} - Q]}{[\text{Ar}][Q]} \quad (2)$$

Here,  $[Ar]$  is the concentration of free naphthalene and  $[Ar-Q]$  is the concentration of the naphthalene– $Ag^+$  complex formed in the ground-state.

Several research groups [4,5,7,8] have proposed the formation of both 1:1 and 2:1 complexes between  $Ag^+$  and aromatic hydrocarbons from cation–aromatic  $\pi$  electron interactions in solution as shown in Scheme 1:



Scheme 1.

For the complexes shown in Scheme 1, Eq. (2) can be rewritten:

$$\begin{aligned} K_S &= \frac{[AgAr^+] + [Ag_2Ar^{2+}]}{([Ag_t^+] - [AgAr^+] - 2[Ag_2Ar^{2+}])([Ar]} \\ &= K_1 + K_1 K_2 [Ag^+] \end{aligned} \quad (3)$$

where  $[Ag_t^+]$  is the total concentration of  $Ag^+$  ions added to the aqueous naphthalene solution. As shown in Eq. (3),  $K_S$  depends on the free concentration of  $Ag^+$  and, because of the stoichiometry for a fixed naphthalene concentration, the initial  $Ag^+$  concentration. For example, the  $K_{S,0.002}$  ( $[Ag^+] = 0.002$  M) value determined from the static and dynamic quenching curves shown in Fig. 2A over the range  $[Ag^+] = 0$  to  $0.004$  M is slightly smaller than  $K_{S,0.004}$  ( $[Ag^+] = 0.004$  M) obtained over the range  $[Ag^+] = 0.002$  to  $0.008$  M. We were thus able to determine different  $K_S$  values for naphthalene as a function of  $Ag^+$  concentration (Fig. 3A) and then calculate the  $Ag^+$  complexation constants  $K_1$  and  $K_2$  directly via linear regression according to Eq. (3) (Table 1).

### 3.3. Dynamic and steady-state fluorescence measurements for pyrene with corrections for pyrene– $Ag^+$ exciplex interference

The primary mechanism responsible for dynamic quenching of PAH fluorescence by  $Ag^+$  ions is intersystem crossing (ISC) to the lowest triplet excited state from the lowest singlet excited state [30]. For naphthalene, ISC alone appears to be the sole quenching mechanism since no exciplex emission was observed in a companion study [31]. Therefore, the fluorescence quenching procedure described above could be used directly to calculate  $Ag^+$  complexation constants for naphthalene. With pyrene, however, exciplex formation [31] resulted in varying degrees of emission interference over the wavelength range of 370–395 nm when using the methodology above (i.e. higher emission intensities, inconsistent with normal dynamic quenching, were observed at those wavelengths). In other words, depending on the emission wavelength monitored, different values of  $K_1$  and  $K_2$  were calculated. The largest impact (i.e. smallest apparent values

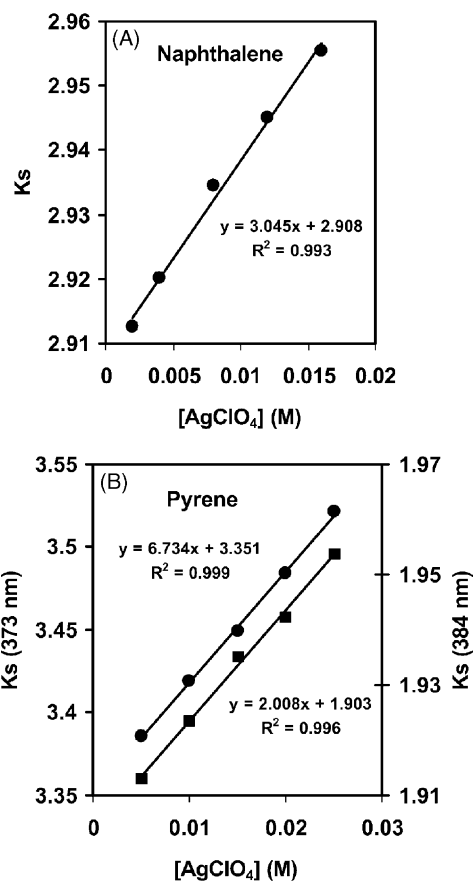


Fig. 3. Representative results for the effect of  $Ag^+$  concentration on the static fluorescence quenching constant,  $K_S$ , for (A) naphthalene ( $[Naph] = 2.0 \times 10^{-4}$  M,  $\lambda_{em} = 322$  nm) and (B) pyrene ( $[Pyr] = 4.5 \times 10^{-7}$  M,  $\lambda_{em} = 373$  nm (●) or 384 nm (■)). Apparent  $Ag^+$  complexation constants  $K_1$  and  $K_2$  can be determined from the intercepts and slopes of the best fit lines according to Eq. (3).

of  $K_1$  and  $K_2$ ) occurred at the wavelengths having the highest exciplex emission intensities. To correct for the exciplex emission interference, it was necessary to apply the procedure described above for naphthalene to pyrene fluorescence at multiple emission wavelengths that exhibited varying degrees of exciplex emission, and then extrapolate these results to the hypothetical condition of no exciplex interference.

In aqueous solution, the pyrene– $Ag^+$  exciplex has a maximum intensity at 379 nm, which can be highlighted by normalizing steady-state fluorescence emission spectra in the presence and absence of  $Ag^+$  at the 0–0 transition of pyrene ( $\lambda_{em} = 373$  nm) [31]. Although this type of normalization clearly distinguishes the presence of the exciplex, multi-wavelength time-resolved fluorescence measurements demonstrate that the exciplex interference also occurs at the 0–0 transition as evidenced by a significant nonzero exciplex preexponential factor and an exciplex emission lifetime consistent with the other wavelengths [31]. For example, fluorescence lifetimes of the pyrene monomer and exciplex ( $\tau_{mo} = 43.30 \pm 1.78$  ns,  $\tau_{exc} = 3.21 \pm 0.84$  ns) measured at the emission wavelength of 373 nm in the presence of

Table 1  
Ag<sup>+</sup> complexation constants<sup>a</sup> for aromatic hydrocarbons in aqueous solution

PAHs	This study		Andrews and Keefer [4]		Kofahl and Lucas [5]		Yim [7]		Zhu et al. [24]	
	$K_1$	$K_2$	$K_1$	$K_2$	$K_1$	$K_2$	$K_1$	$K_2$	$K_1$	$K_2$
Benzene	nd <sup>b</sup>	nd	2.41 <sup>d</sup>	0.212 <sup>d</sup>	nd	nd	nd	nd	2.26 <sup>h</sup>	nd
Naphthalene	2.908 (0.092) <sup>c</sup>	1.046 (0.064) <sup>c</sup>	3.080 <sup>d</sup>	0.909 <sup>d</sup>	3.212 <sup>e</sup> 2.937 <sup>e</sup> 2.726 <sup>f</sup>	0.966 <sup>e</sup> 0.909 <sup>e</sup> 0.866 <sup>f</sup>	2.990 <sup>g</sup>	0.378 <sup>g</sup>	nd	nd
Phenanthrene	nd	nd	3.670 <sup>d</sup>	1.800 <sup>d</sup>	3.550 <sup>d</sup>	0.990 <sup>d</sup>	nd	nd	nd	nd
Pyrene	3.965 (0.144) <sup>c</sup>	2.349 (0.156) <sup>c</sup>	nd	nd	nd	nd	3.615 <sup>g</sup>	1.261 <sup>g</sup>	nd	nd
Perylene	nd	nd	nd	nd	nd	nd	4.034 <sup>g</sup>	1.255 <sup>g</sup>	nd	nd

<sup>a</sup> Units for  $K_1$  and  $K_2$  are M<sup>-1</sup> and M<sup>-2</sup>, respectively.

<sup>b</sup> nd, not determined.

<sup>c</sup> Determined by fluorescence quenching at room temperature ( $21 \pm 2^\circ\text{C}$ ),  $I = 0.1\text{ M}$ . Average values and standard errors (in parentheses) were determined from three independent replicate experiments.

<sup>d</sup> Determined by solubility enhancement at  $25^\circ\text{C}$ ,  $I = 1.0\text{ M}$ .

<sup>e</sup> Determined by solubility enhancement at  $20^\circ\text{C}$ ,  $I = 1.0\text{ M}$ .

<sup>f</sup> Determined by solubility enhancement at  $30^\circ\text{C}$ ,  $I = 1.0\text{ M}$ .

<sup>g</sup> Determined by solubility enhancement at  $20^\circ\text{C}$ ,  $I$  varied with AgClO<sub>4</sub> concentration added.

<sup>h</sup> Determined by deuterium nuclear magnetic resonance relaxation at  $19^\circ\text{C}$ ,  $I$  varied with AgNO<sub>3</sub> concentration added.

5.0 mM AgClO<sub>4</sub> are consistent with the average values ( $\tau_{\text{mo}} = 44.54 \pm 2.05\text{ ns}$ ,  $\tau_{\text{exc}} = 3.42 \pm 0.34\text{ ns}$ ) determined at other emission wavelengths (379, 383, and 393 nm) within the limits of measurement error. However, ratios between the exciplex and monomer preexponential factors ( $A_{\text{exc}}/A_{\text{mo}}$ ) at these different emission wavelengths are different from one another, with the smallest and highest ratios being observed at 373 and 379 nm, respectively, as expected [31]. From these  $A_{\text{exc}}/A_{\text{mo}}$  ratios and their corresponding apparent  $K_1$  and  $K_2$  values computed at each wavelength, we could then establish trends that enabled us to extrapolate Ag<sup>+</sup> complexation constants free of the exciplex interference (Figs. 2B, 3B and 4; Table 1).

### 3.4. Comparison with literature values

The Ag<sup>+</sup> complexation constants determined here for pyrene are larger than those we measured for naphthalene (Table 1), consistent with previous observations [4,5,7]. For example, Yim [7] has suggested that  $K_1$  and  $K_2$  values should increase proportionally with increasing PAH size and reduction potential up to some maximum  $K_1$  and  $K_2$  values; beyond these limits,  $K_1$  and  $K_2$  values would either be relatively constant or might actually decrease slightly with increasing PAH size. In addition, it can be seen from the values in Table 1 that the Ag<sup>+</sup> complexation constants we determined for naphthalene and pyrene via fluorescence quenching are reasonably consistent with previously reported literature values for these and other aromatic hydrocarbons [4,5,7,24]. Likely explanations for the slight differences observed include different experimental conditions and procedures. For example, our study was performed at room temperature ( $21 \pm 2^\circ\text{C}$ ), whereas most of the previous work was done at  $25^\circ\text{C}$  with the exception of Yim [7] ( $20^\circ\text{C}$ ), Zhu et al. [24] ( $19^\circ\text{C}$ ), and Kofahl and Lucas [5] who determined Ag<sup>+</sup> complexation constants for naphthalene over the temperature range  $20\text{--}30^\circ\text{C}$ . The largest experimental difference, however, was our use of fluorescence quenching techniques that enabled us to work at much lower Ag<sup>+</sup> concentrations and a much lower and constant ionic strength ( $I = 0.1\text{ M}$ ) compared to previous workers who utilized solubility enhancement [4,5,7,8] or NMR [24] methodologies. For example, Yim [7] has explained that the constant ionic medium ( $I = 1.0\text{ M}$ ) solubility enhancement approach used by Andrews and Keefer [4] and Kofahl and Lucas [5] overestimates Ag<sup>+</sup> complexation constants because it does not take into consideration PAH salting out by KNO<sub>3</sub>, which is particularly important for the solubility measurement in the

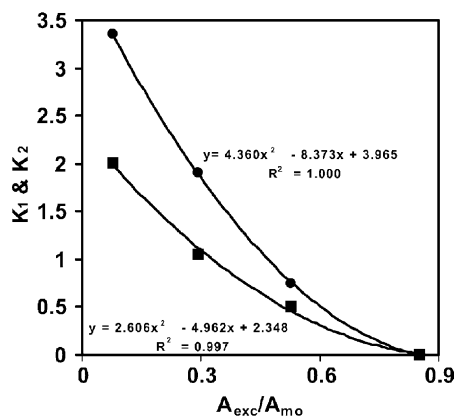


Fig. 4. Representative trendlines established for the pyrene exciplex–monomer preexponential factor ratios ( $A_{\text{exc}}/A_{\text{mo}}$ ) and apparent Ag<sup>+</sup> complexation constants  $K_1$  (●) and  $K_2$  (■). Experimental conditions: [Pyr] =  $4.5 \times 10^{-7}\text{ M}$ , [Ag<sup>+</sup>] = 5.0 mM,  $I = 0.1\text{ M}$ . Specific values shown above are  $A_{\text{exc}}/A_{\text{mo}}(\lambda_{\text{em}}) = 0.075$  (373 nm), 0.294 (384 nm), 0.528 (393 nm), 0.852 (379 nm).



absence of  $\text{AgNO}_3$ . Conversely, although the variable ionic strength approach utilized by Yim [7] and Zhu et al. [24] does not suffer to the same degree from salting out effects, its major weakness is the inability to maintain constant solution activity coefficients with increasing  $\text{Ag}^+$  concentrations. Because the fluorescence quenching technique developed here does not rely on a macroscopic solubility enhancement measurement nor high concentrations of PAH molecules and  $\text{Ag}^+$  ions, we were able to maintain a low and constant ionic strength condition which circumvented these particular problems. It should also be noted that the fluorescence quenching technique is inherently faster and more sensitive than the solubility enhancement methodology, because it does not require (1) establishment of a solid PAH phase that is in equilibrium with PAH molecules dissolved in an aqueous solution, (2) high-speed centrifugation to separate PAH crystals from solution, and (3) quantification of the dissolved phase PAH concentration. In addition, because relatively small solution volumes and very low concentrations of  $\text{Ag}^+$  and PAHs can be used with the fluorescence quenching procedure, there is less chemical waste generated.

#### 4. Conclusions

Using steady-state and time-resolved fluorescence quenching methods, we have demonstrated that complexation constants ( $K_1$  and  $K_2$ ) for the 1:1 and 2:1 complexes formed from the reaction between  $\text{Ag}^+$  and PAH molecules can be readily determined. For PAH molecules (e.g. naphthalene) that do not form exciplexes with  $\text{Ag}^+$ ,  $K_1$  and  $K_2$  values can be determined directly with Eq. (3). However, if PAH molecules (e.g. pyrene) form exciplexes that interfere with the monomer emission, additional steps are needed to extrapolate  $K_1$  and  $K_2$  values from the data. The novel approach developed here to quantify ground-state PAH complexes with  $\text{Ag}^+$  should work equally well for characterizing complexes formed between other organic fluorescent molecules and metal cations. In particular, since other routine spectroscopic techniques such as UV-Vis absorption,  $^1\text{H}$  NMR, and FTIR are often unable to quantify these types of weak interactions in aqueous solutions because of their relative insensitivities, the fluorescence quenching methodology described here offers new opportunities to investigate weak metal–organic complexes (e.g. those resulting from cation– $\pi$  interactions).

#### Acknowledgements

We gratefully acknowledge the National Science Foundation (CTS 0096053) for providing the financial support for this study.

#### References

- [1] A.E. Hill, *J. Am. Chem. Soc.* 43 (1921) 254.
- [2] A.E. Hill, *J. Am. Chem. Soc.* 44 (1922) 1163.
- [3] A.E. Hill, F.W. Miller, *J. Am. Chem. Soc.* 47 (1925) 2702.
- [4] L.J. Andrews, R.M. Keefer, *J. Am. Chem. Soc.* 71 (1949) 3644.
- [5] R.E. Kofahl, H.J. Lucas, *J. Am. Chem. Soc.* 76 (1954) 3931.
- [6] Y. Nosaka, A. Kira, M. Imamura, *J. Phys. Chem.* 85 (1981) 1353.
- [7] S. Yim, Ph.D. Dissertation, Texas A&M University, College Station, TX, 2001.
- [8] N. Ogimachi, L.J. Andrews, R.M. Keefer, *J. Am. Chem. Soc.* 78 (1956) 2210.
- [9] H. Masuhara, H. Shioyama, T. Saito, K. Hamada, S. Yasoshima, N. Mataga, *J. Phys. Chem.* 88 (1984) 5868.
- [10] N.L. Ma, K.M. Ng, C.W. Tsang, *Chem. Phys. Lett.* 277 (1997) 306.
- [11] K.M. Ng, N.L. Ma, C.W. Tsang, *Rapid Commun. Mass. Spectrom.* 12 (1998) 1679.
- [12] H.G. Smith, R.E. Rundle, *J. Am. Chem. Soc.* 80 (1958) 5075.
- [13] E.A. Hall, E.L. Amma, *J. Am. Chem. Soc.* 91 (1969) 6538.
- [14] E.A.H. Griffith, E.L. Amma, *J. Am. Chem. Soc.* 96 (1974) 743.
- [15] E.A.H. Griffith, E.L. Amma, *J. Am. Chem. Soc.* 96 (1975) 5407.
- [16] S. Mecozzi, A.P. West, D.A. Dougherty, *J. Am. Chem. Soc.* 118 (1996) 2307.
- [17] M. Munakata, L.P. Wu, T. Kuroda-Sowa, M. Maekawa, Y. Suenaga, K. Sugimoto, *Inorg. Chem.* 36 (1997) 4903.
- [18] M. Munakata, L.P. Wu, T. Kuroda-Sowa, M. Maekawa, Y. Suenaga, G.L. Ning, T. Kojima, *J. Am. Chem. Soc.* 120 (1998) 8610.
- [19] R.S. Mulliken, *J. Am. Chem. Soc.* 74 (1952) 811.
- [20] K. Fukui, A. Imamura, T. Yonezawa, C. Nagata, *Bull. Chem. Soc. Jpn.* 34 (1961) 1076.
- [21] M. Munakata, L.P. Wu, G.L. Ning, *Coord. Chem. Rev.* 198 (2000) 171.
- [22] T. Kubota, H. Miyazaki, K. Ezumi, M. Yamakawa, *Bull. Chem. Soc. Jpn.* 47 (1974) 491.
- [23] T. Kubota, K. Kano, B. Uno, T. Konse, *Bull. Chem. Soc. Jpn.* 60 (1987) 3865.
- [24] D. Zhu, B.E. Herbert, M.A. Schlautman, E.R. Carraway, *J. Environ. Qual.* (in press).
- [25] A.R. Watkins, *J. Phys. Chem.* 77 (1973) 1207.
- [26] T.D. Gauthier, E.C. Shane, W.D. Guerin, W.R. Seitz, C.L. Grant, *Environ. Sci. Technol.* 20 (1986) 1162.
- [27] J.R. Lakowicz, *Principles of Fluorescence Spectroscopy*, second ed., Kluwer Academic/Plenum Publisher, New York, 1999.
- [28] T. Nakamura, A. Kira, M. Imamura, *J. Phys. Chem.* 86 (1982) 3359.
- [29] S.V. Linderman, R. Linderman, J.K. Kochi, *Inorg. Chem.* 39 (2000) 5707.
- [30] R.H. Hoffldt, R. Sahai, S.H. Lin, *J. Chem. Phys.* 53 (1970) 4512.
- [31] J.H. Lee, M.A. Schlautman, E.R. Carraway, S. Yim, B. E. Herbert, *J. Photochem. Photobiol. A*, submitted for publication.